Research Paper

CircUBAP2-mediated competing endogenous RNA network modulates tumorigenesis in pancreatic adenocarcinoma

Rongjie Zhao[1,*], Junjie Ni[2,*], Si Lu[3,*], Sujing Jiang[4], Liangkun You[1], Hao Liu[1], Jiawei Shou[1], Chongya Zhai[1], Wei Zhang[1], Shengpeng Shao[5], Xinmei Yang[6], Hongming Pan[1], Weidong Han[1]

[1]Department of Medical Oncology, Sir Run Run Shaw Hospital, College of Medicine, Zhejiang University, Hangzhou 310000, Zhejiang, China
[2]The First Clinical College, Zhejiang Chinese Medical University, Hangzhou 310053, Zhejiang, China
[3]The Fourth Clinical College, Zhejiang Chinese Medical University, Hangzhou 310053, Zhejiang, China
[4]Department of Radiation and Medical Oncology, The First Affiliated Hospital of Wenzhou Medical University, Wenzhou 325000, Zhejiang, China
[5]The Second Clinical College, Zhejiang Chinese Medical University, Hangzhou 310053, Zhejiang, China
[6]Department of Oncology, The First Affiliated Hospital of Jiaxing University, Jiaxing 314000, Zhejiang, China
*Equal contribution

Correspondence to: Weidong Han, Hongming Pan; **email:** hanwd@zju.edu.cn, panhongming@zju.edu.cn
Keywords: pancreatic adenocarcinoma, circRNA, ceRNA, immune microenvironment
Received: July 30, 2019 **Accepted:** September 22, 2019 **Published:** October 4, 2019

ABSTRACT

We investigated the role of the competing endogenous RNA (ceRNA) network in the development and progression of pancreatic adenocarcinoma (PAAD). We analyzed the expression profiles of PAAD and normal pancreatic tissues from multiple GEO databases and identified 457 differentially expressed circular RNAs (DEcircRNAs), 19 microRNAs (DEmiRNAs) and 1993 mRNAs (DEmRNAs). We constructed a ceRNA network consisting of 4 DEcircRNAs, 3 DEmiRNAs and 149 DEmRNAs that regulates the NF-kappa B, PI3K-Akt, and Wnt signaling pathways. We then identified and validated five hub genes, *CXCR4*, *HIF1A*, *ZEB1*, *SDC1* and *TWIST1*, which are overexpressed in PAAD tissues. The expression of *CXCR4*, *HIF1A*, *ZEB1,* and *SDC1* in PAAD was regulated by *circ-UBAP2* and *hsa-miR-494*. The expression of *CXCR4* and *ZEB1* correlated with the levels of M2 macrophages, T-regulatory cells (Tregs) and exhausted T cells in the PAAD tissues. The expression of *CXCR4* and ZEB1 positively correlated with the expression of *CTLA-4* and *PD-1*. This suggests that *CXCR4* and *ZEB1* proteins inhibit antigen presentation and promote immune escape mechanisms in PAAD cells. In summary, our data suggest that the *circUBAP2*-mediated ceRNA network modulates PAAD by regulating the infiltration and function of immune cells.

INTRODUCTION

Pancreatic adenocarcinoma (PAAD) is the most commonly occurring pancreatic cancer, and the seventh leading cause of tumor-related death in both men and women worldwide [1]. It is often asymptomatic during the early stages. Although the treatment of PAAD has improved in recent years, thanks to the availability of newer chemotherapeutic drugs and advances in surgical techniques, the survival rates of PAAD patients remain very low. The majority of the patients are diagnosed with advanced stage PAAD, which is not amenable for surgical therapy [2]. Moreover, the 5-year survival rates of patients that have undergone successful surgery remain below 8% because of disease recurrence [3]. In addition, high rates of drug resistance to several chemotherapeutic drugs, including gemcitabine also contribute to low survival rates [4]. Therefore, reliable biomarkers useful for accurate early diagnoses are needed to improve survival rates in patients with PAAD.

Previous studies have revealed several protein-coding genes, miRNAs or long non-coding RNAs (lncRNAs) that regulate PAAD. For example, upregulation of *miR-222* promotes tumor cell proliferation and invasiveness in PAAD by decreasing the nuclear levels of the *p27* tumor suppressor protein [5]. In addition, silencing *LINC00958* prevents initiation of pancreatic tumorigenesis by inhibiting *PAX8* via *miR-330-5p* [6]. Circular RNAs (circRNAs) are a novel class of endogenous small non-coding RNAs that form covalently closed-loop structures and lack a 5′ cap or 3′ poly-A tail [7]. Although previously thought to be generated as a result of splicing errors [8], recent advances in RNA sequencing technologies have revealed that they play a key role in regulating gene expression by sponging miRNAs [9]. Aberrant expression of circRNAs has been documented in several human diseases, including cancers [10].

The exosomes secreted by PAAD cells contain circular aminoacyl-tRNA synthetases (*circ-IARS)*, which promote tumor invasion and metastasis by enhancing endothelial monolayer permeability [11]. A competing endogenous RNA (ceRNA) network that includes circRNAs and miRNAs plays a critical role in posttranscriptional regulation of key proteins, and dysregulation of ceRNAs is associated with tumor development and progression [12]. However, the role of circRNAs in the growth and progression of PAAD is not fully understood [13]. The immune system plays a crucial role in PAAD growth and progression [14]. For that reason, we investigated the relationship between ceRNAs and tumor-infiltrated immune cells in the development and progression of PAAD.

RESULTS

Identification of DEcircRNAs, DEmiRNAs, and DEmRNAs in PAAD tissues

We normalized the expression of circRNAs (Supplementary Figures 1A and 1B), microRNAs and mRNAs (Supplementary Figures 1C and 1D) in PAAD and normal pancreatic tissues. We identified 457 differentially expressed circRNAs (DEcircRNAs), which included 174 in the GSE69362 dataset [15] and 283 in the GSE79634 dataset [16], based on a threshold of P value < 0.05 and $|\log FC| \geq 1$. We generated volcano plots and heatmaps of the DEcircRNAs (Figures 1A and 1B), 19 DEmiRNAs (7 up-regulated and 12 down-regulated; Figure 1C) and 1993 DEmRNAs (1012 up-regulated and 981 down-regulated; Figure 1D) to demonstrate their aberrant expression in PAAD tissues. We compared the DEcircRNAs from the two datasets and identified 19 up-regulated and 8 down-regulated DEcircRNAs for further analysis (Figure 1E).

Construction of the circRNA-miRNA-mRNA network

We analyzed the DEcircRNAs, DEmiRNAs and DEmRNAs using the CSCD database and identified circRNA-miRNA pairs. We also identified miRNA-mRNA pairs by analyzing the miRDB, miRTarBase and TargetScan databases (Figure 1F). Finally, we generated a ceRNA network that consisted of 4 DEcircRNAs (*circ-HIBADH*, *circ-UBAP2*, *circ-TADA2A* and *circ-CLEC17A*), 3 DEmiRNAs (*has-miR-214*, *has-mir-324-3p and has-miR-494*) and 149 DEmRNAs using the Cytoscape software as shown in Figure 2. The basic characteristics of the 4 DEcircRNAs are shown in Table 1 and Figure 3. Furthermore, we found that *circ-CLEC17A* is aberrantly overexpressed in PAAD tissues from females compared to males (Supplementary Figures 2A–2D).

Analysis of DEmRNAs

We performed Gene ontology (GO) and Kyoto Encyclopedia of Genes and Genomes (KEGG) analyses of the DEmRNAs to identify aberrantly regulated biological processes and signaling pathways in PAAD. The Gene Ontology analyses suggested that biological processes such as cell proliferation, angiogenesis and negative regulation of transcription from RNA polymerase II promoter were dysregulated (Figure 4A). KEGG pathway analysis of DEmRNAs highlighted the involvement of the NF-kappa B, PI3K-Akt, and Wnt signaling pathways, and cancer-related dysregulation of transcription (Figure 4B). The NF-kappa B, PI3K-Akt, and Wnt signaling pathways have previously been implicated in the growth and progression of PAAD [17–19]. The Sankey plots for all the enriched GO terms and KEGG pathways with a P value < 0.05 were shown, further highlighting the genes and the pathways involved in PAAD.

Identification and validation of the hub genes

We analyzed the DEmRNAs using the Search Tool for the Retrieval of Interacting Genes database (STRING) and constructed a protein-protein interaction (PPI) network consisting of 141 nodes and 50 edges (Figure 5). We identified the top 15 genes, which were found in at least 6/11 topological algorithms and had a high-ranking score. After integrating the results of the GO, KEGG and PPI network analyses, we identified 5 hub genes that were closely related to PAAD tumorigenesis, namely, C-X-C Motif Chemokine Receptor 4 (*CXCR4*), Hypoxia-Inducible Factor 1 Subunit Alpha (*HIF1A*), Zinc Finger E-Box Binding Homeobox 1 (*ZEB1*), Syndecan 1 (*SDC1*) and Twist Family BHLH Transcription Factor 1 (*TWIST1*).

The transcription levels of the 5 hub genes in GSE60980 (GPL14550), 3 related miRNAs in GSE60980 (GPL15159), and 4 circRNAs in GSE79634 (Figure 6) and GSE69362 (Supplementary Figure 3) were shown. We further validated the 5 hub genes by analyzing their mRNA expression in the Gene Expression Profiling Interactive Analysis (GEPIA) and the protein expression in The Human Protein Atlas (THPA) database as shown in Figures 7A and 7B, respectively. The transcription levels of these 5 hub genes in GEPIA were similar to the results in Figure 6. The protein expression data in the THPA database showed that *SDC1* and *ZEB1* were aberrantly overexpressed in PAAD compared to normal pancreatic tissues, which were in accordance with our transcription results in Figure 6. However, *HIF1A* protein levels were low in both PAAD and normal pancreatic tissues, and the protein levels of the remaining two hub proteins, *CXCR4* and *TWIST1* were not found in the THPA database.

Analysis of prognosis and tumor infiltration of immune cells

We analyzed the overall survival (OS) using the Kaplan-Meier Plotter database (KM plotter database) to determine the prognostic value of hub genes and

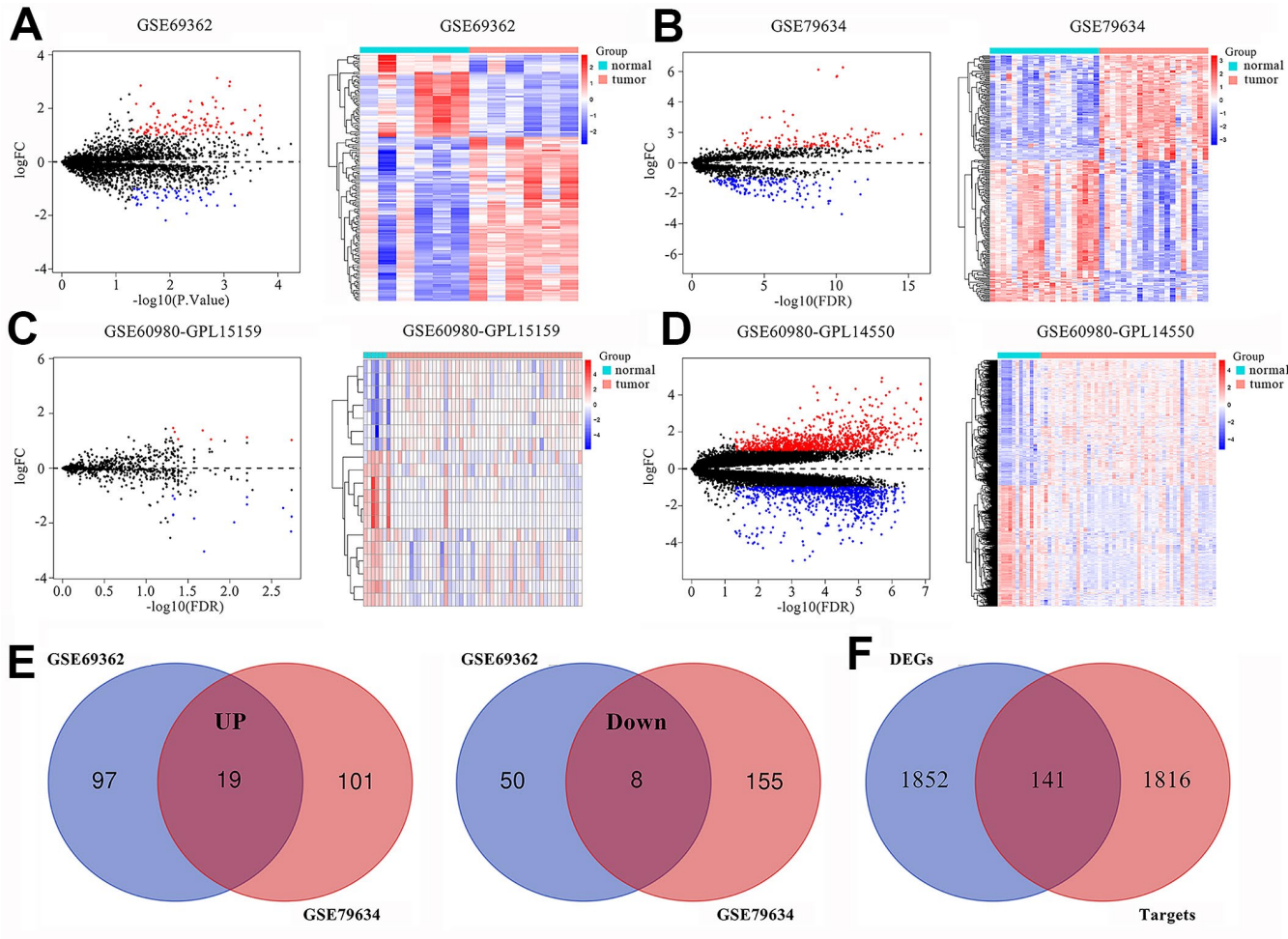

Figure 1. Differentially expressed circRNAs, miRNAs and mRNAs in pancreatic adenocarcinomas (PAAD). Volcano plots and heatmaps show identification of (**A**) DEcircRNAs in GSE69362, (**B**) DEcircRNAs in GSE79634, (**C**) DEmiRNAs in GSE60980 (GPL15159) and (**D**) DEmRNAs in GSE60980 (GPL14550) between PAAD tissues and adjacent normal pancreatic tissue. The red color indicates upregulated genes in the PAAD tissues and blue color indicates downregulated genes, while black color indicates genes with no significant differences between the PAAD and normal pancreatic tissues. Heatmaps show the expression patterns of DEcircRNAs, DEmiRNAs and DEmRNAs. The PAAD and adjacent normal pancreatic tissues are represented by red and blue color, respectively. (**E**) Venn diagrams show commonly upregulated DEcircRNAs and downregulated DEcircRNAs in the PAAD tissues in both GSE69362 and GSE79634. Purple and orange circles indicate the number of DEcircRNAs in the GSE69362 and GSE79634 datasets, respectively. The red circles in the middle indicate the overlapping circRNAs between the two datasets. (**F**) Venn diagram shows the intersection between DEmiRNA-predicted targets obtained from miRDB, miRTarBase and TargetScan databases and DEmRNAs in GSE60980 (GPL14550).

miRNAs. Prognosis based on their high and low expression in PAAD tissues is shown in Figure 8. High expression of *SDC1* and *TWIST1* was associated with poorer OS (HR = 2.23, *P* = 0.0030 and HR = 1.66, *P* = 0.018). High expression of *hsa-miR-494* and *hsa-miR-324* was associated with increased OS (HR = 0.64, *P* = 0.033 and HR = 0.50, *P* = 0.00095).

Since several studies have shown that immune cell infiltration and the tumor microenvironment plays a critical role in the development of cancers, we analyzed the relationship between the expression of the hub genes and the status of immune cell infiltration in PAAD tumors using the Tumor Immune Estimation Resource (TIMER) database. As shown in Supplementary Figure 4, *CXCR4* expression positively correlated with the infiltration levels of B cells (Cor = 0.401, *P* = 5.40e-08), CD4+ T cells (Cor = 0.435, *P* = 3.56e-09), neutrophils (Cor = 0.496, *P* = 5.46e-12), macrophages (Cor = 0.467, *P* = 1.20e-10), and dendritic cells or DCs (Cor = 0.503, *P* = 2.40e-12). *ZEB1* expression positively correlated with infiltration levels of CD8+ T cells (Cor = 0.525, *P* = 1.59e-13), neutrophils (Cor = 0.519, *P* = 3.44e-13), macrophages (Cor = 0.693, *P* = 8.68e-26), and DCs (Cor = 0.572, *P* = 3.09e-16). However, *SDC1* expression showed no significant correlation with immune cell infiltration in the PAAD tumors. These results suggested that the circRNA-mediated ceRNAs might modulate tumorigenesis by regulating the infiltration of immune cells in PAAD.

Correlation analysis between the hub genes and the immune cell markers

Next, to further characterize the role of the different subsets of immune cells with PAAD tumorigenesis, we analyzed the correlation between the expression of hub genes and various immune cell markers, including markers specific for CD8+ T cells, T cells (general), B cells, monocytes, tumor-associated macrophages (TAMs), M1 and M2 macrophages, neutrophils, natural killer cells (NKs) and DCs. We also analyzed the data for different subsets of T cells, such as T-helper 1 (Th1) cells, T-helper 2 (Th2) cells, follicular helper T cells (Tfhs), T-helper 17 cells (Th17s), regulatory T cells (Tregs) and exhausted T cells. After adjusting for purity, we found that the expression of most of the immune cell markers positively correlated with the expression of *CXCR4* and *ZEB1* and negatively correlated with *SDC1* expression in PAAD tissues (Table 2).

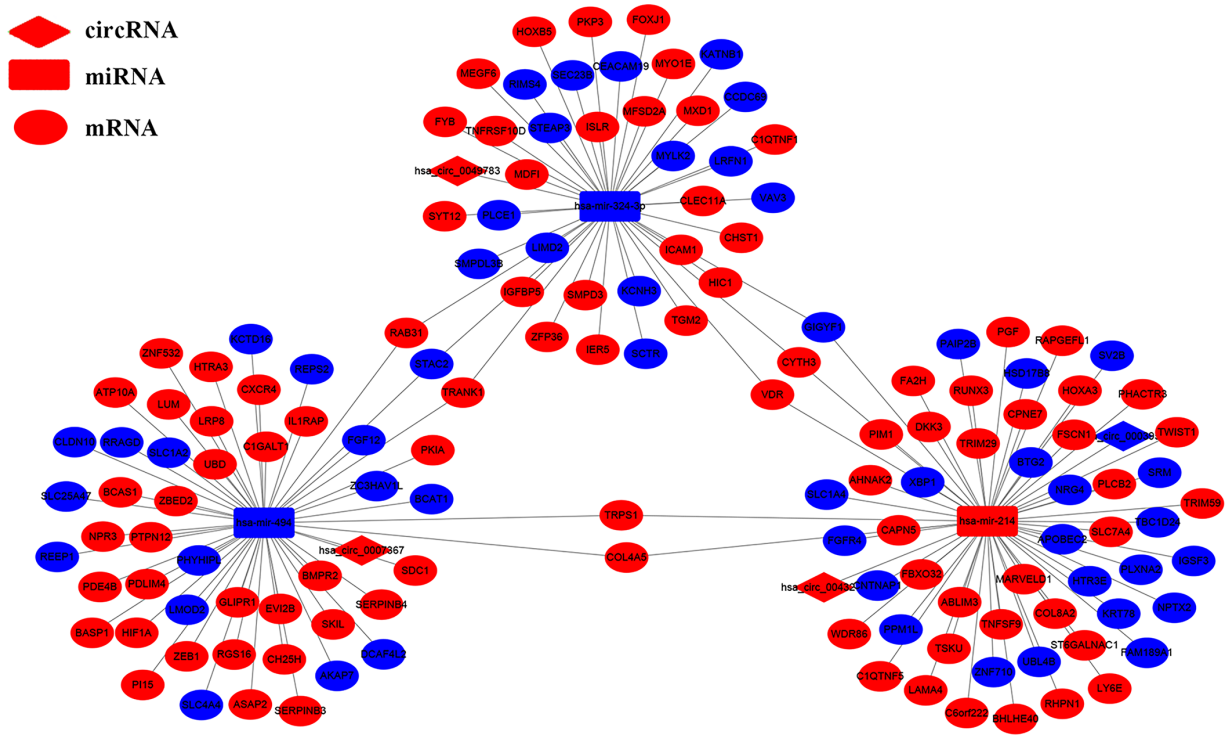

Figure 2. The circRNA-miRNA-mRNA interaction network in the PAAD tissues. The circRNA-miRNA-mRNA interaction network consists of 4 circRNAs (*hsa_circ_0007367*, *hsa_circ_0003958*, *hsa_circ_0043278* and *hsa-circ-0049783*), 3 miRNAs (*hsa-mir-324-3p*, *hsa-miR-214* and *hsa-miR-494*), and 149 mRNAs. The diamond nodes indicate the circRNAs; rectangle nodes indicate the miRNAs; the elliptical nodes indicate the mRNAs. The edges indicate a possible connection between the circRNAs, miRNAs, and the mRNAs. The red and blue color indicates high and low expression of the ceRNAs in the PAAD tissues, respectively.

Table 1. Basic characteristics of the 4 differently expressed circRNAs.

CircRNA	Log2FC	Regulation	Type	Chromosome	Strand	Gene symbol
hsa_circ_0049783	1.35	UP	exonic	chr19	+	*CLEC17A*
hsa_circ_0007367	1.34	UP	exonic	chr9	-	*UBAP2*
hsa_circ_0003958	1.01	DOWN	exonic	chr7	-	*HIBADH*
hsa_circ_0043278	1.19	UP	exonic	chr17	+	*TADA2A*

Log2FC means that log2 transformation to fold changes of circRNA expression between PAAD tissues and normal tissues. UP means upregulated circRNA in PAAD tissues. DOWN means downregulated circRNA in PAAD tissues.

The expression of specific markers for TAMs, M2 macrophages, monocytes and Tregs show a moderate to strong positive correlation with the expression of *CXCR4* and *ZEB1* (Table 2). These include TAM markers such as *CCL-2*, *CD68* and *IL10*, and M2 phenotype markers such as *CD163*, *VSIG4* and *MS4A4A* (Figure 9A–9H). Furthermore, the expression of specific markers for CD8+ T cells, T cells (general) and B cells show a strong

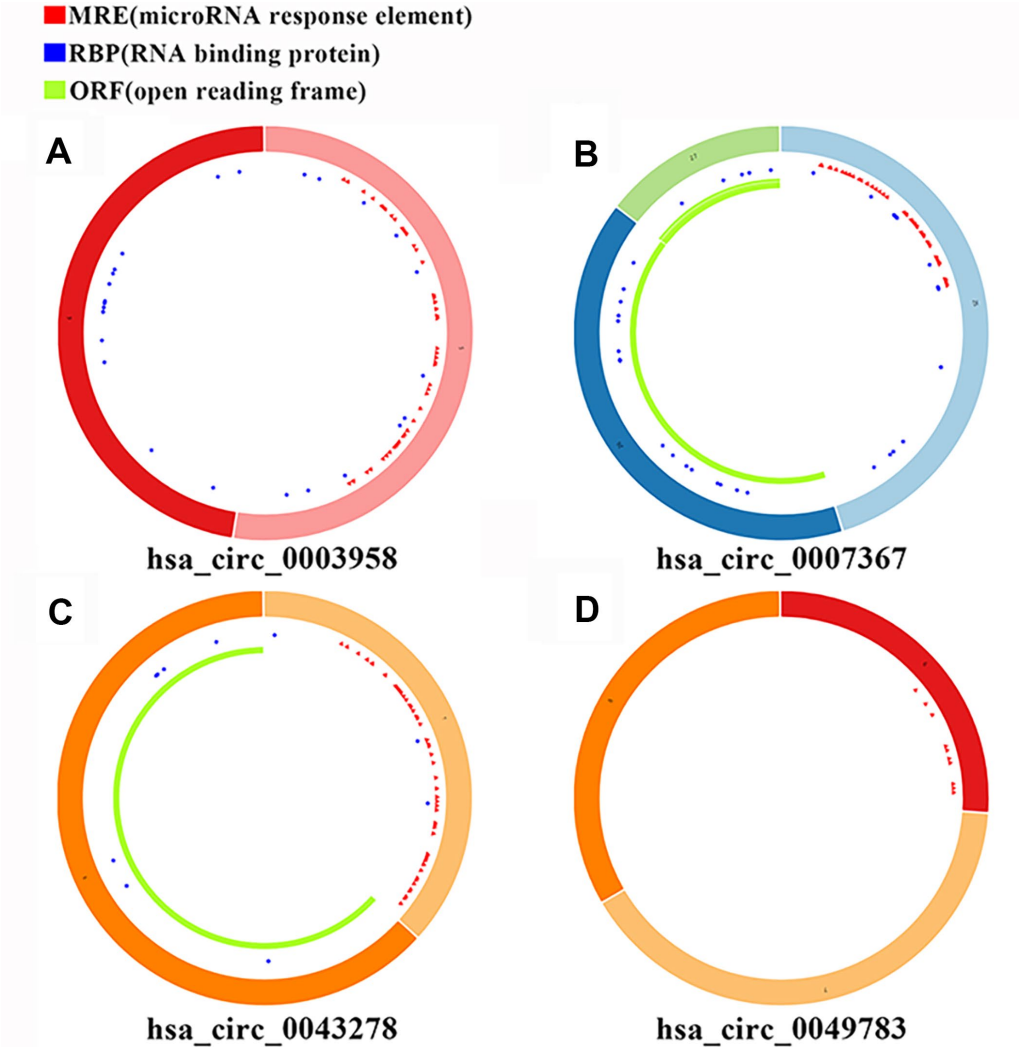

Figure 3. Basic structural features of the 4 PAAD-specific circRNAs. The structural features of (**A**) *hsa_circRNA_0003958*, (**B**) *hsa_circRNA_0007367*, (**C**) *hsa_circRNA_0043278*, and (**D**) *hsa_circRNA_0049783* downloaded from the Cancer-Specific CircRNA Database (CSCD) are shown. The microRNA response element (MRE) is shown in red; The RNA binding protein (RBP) is shown in blue; The open reading frame (ORF) is shown in green.

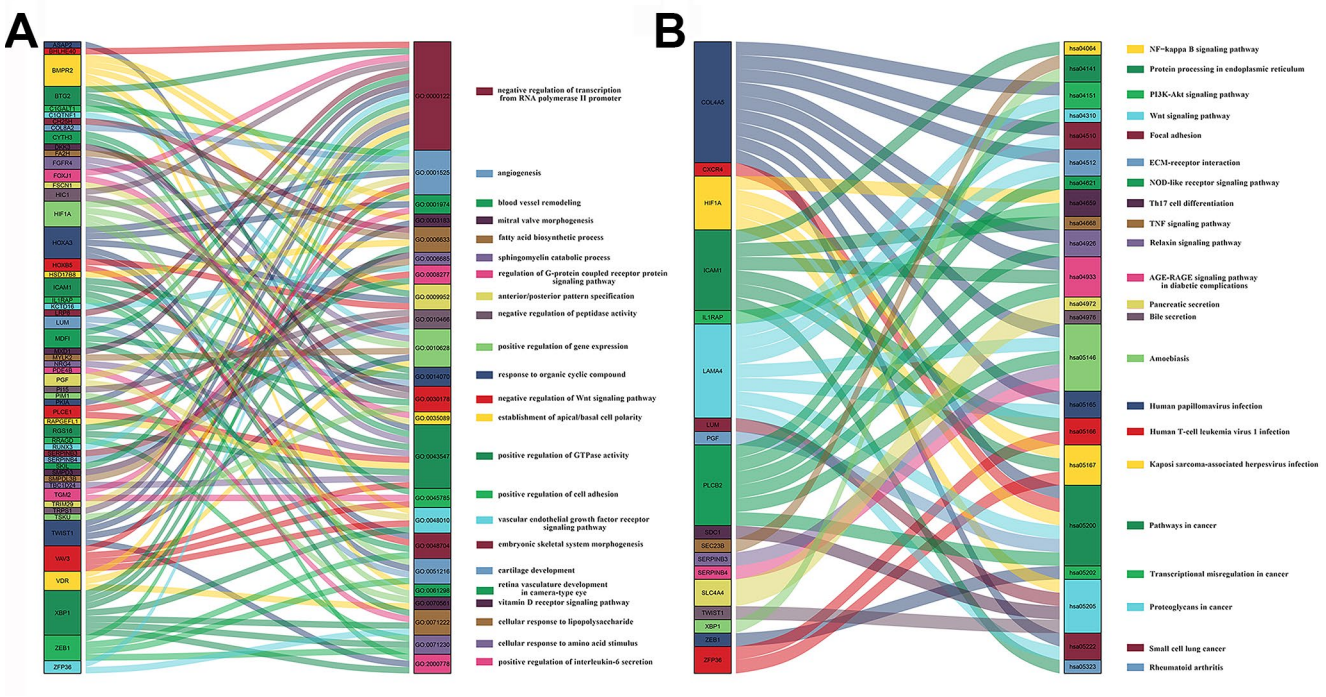

Figure 4. Sankey plots of signaling pathways and biological processes related to differentially expressed mRNAs in PAAD tissues. Sankey plots show (**A**) signaling pathways and (**B**) biological processes (BP) related to DEmRNAs involved in PAAD based on Kyoto Encyclopedia of Genes and Genomes (KEGG) enrichment and Gene Ontology_Biological Process (GO_BP) analyses, respectively.

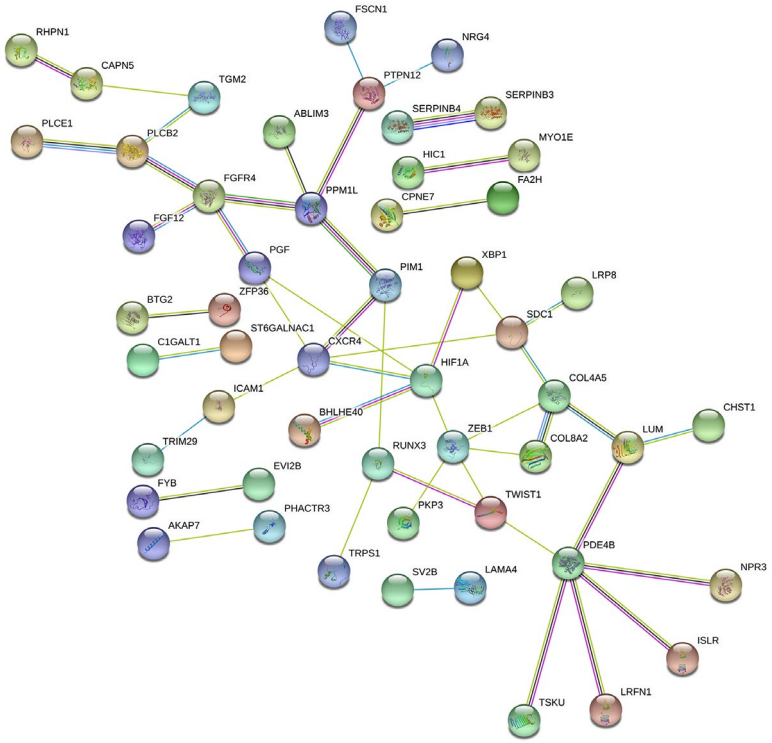

Figure 5. Protein-protein intersection (PPI) network analyses of the DEmRNAs involved in the ceRNA network. The PPI network consists of 141 edges and 50 nodes representing proteins and interactions, respectively. The relative thickness of the edges represents the degree of relationship (weak, moderate, or strong) between the nodes.

positive correlation with the expression of *CXCR4* (Table 2). The high expression of DC markers, *HLA-DPB1*, *HLA-DQB1*, *HLA-DRA*, *HLA-DPA1*, *BDCA-1*, *BDCA-4* and *CD11c* correlates with increased expression of *CXCR4* (P <0.001) and *ZEB1* (P <0.001) (Table 2). This suggests that PAAD cells expressing high levels of *CXCR4* and *ZEB1* proteins might promote DC infiltration. We also observed positive correlation between *CXCR4* and markers of T cell exhaustion, such as programmed cell death protein 1 (*PD-1*), cytotoxic T lymphocyte-associated antigen-4 (*CTLA4*), lymphocyte-activation gene 3 (*LAG3*), T cell immunoglobulin domain and mucin domain-3 (*TIM-3*), and Granzyme B (*GZMB*) (P <0.001) (Table 2).

DISCUSSION

Complex mechanisms involving several genes and pathways are involved in the growth and progression of PAAD. The ceRNA network has emerged a novel method of posttranscriptional gene regulation. In the present study, we identified a total of 457 DEcircRNAs in GSE69362 and GSE79634, 19 DEmiRNAs in GSE60980 (GPL15159) and 1993 DEmRNAs in GSE60980 (GPL14550). We generated a circRNA-mediated ceRNA network that included 4 circRNAs, 3 miRNAs and 149 mRNAs. We then constructed a PPI network and identified 5 hub genes, including *CXCR4*, *HIF1A*, *ZEB1*, *SDC1* and *TWIST1*, by performing

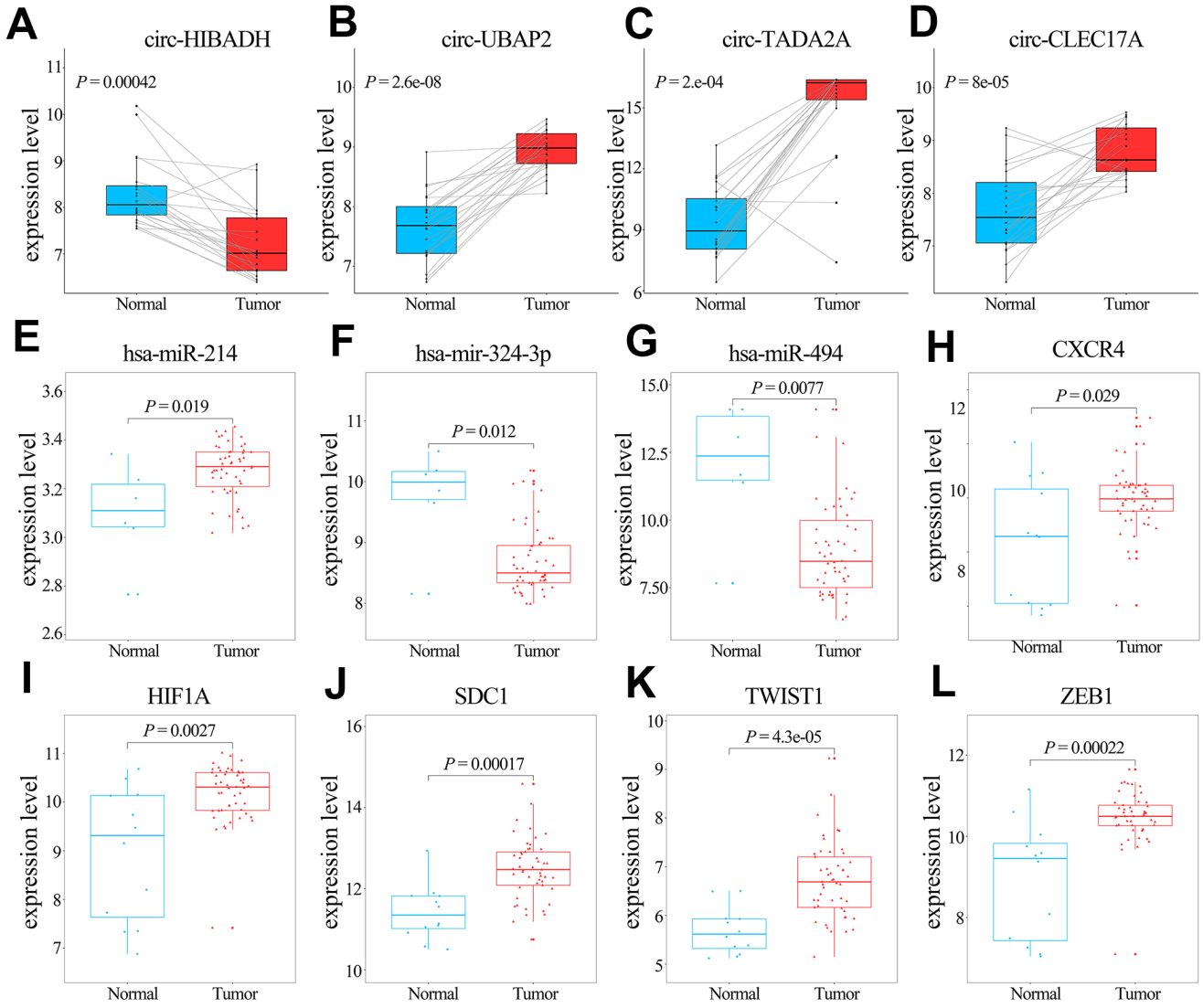

Figure 6. Comparative analyses of the transcription levels of hub genes in GSE60980 (GPL14550), and related miRNAs in GSE60980 (GPL15159) and circRNAs in GSE79634 between PAAD and normal pancreatic tissues. (**A**–**K**) Transcription levels of *circ-HIBADH*, *circ-UBAP2*, *circ-TADA2A*, *circ-CLEC17A*, *hsa-miR-214*, *hsa-mir-324-3p*, *hsa-miR-494*, *CXCR4*, *HIF1A*, *SDC1*, *TWIST1* and *ZEB1* between PAAD (red) and normal pancreatic tissues (blue).

functional enrichment using GO and KEGG pathway analyses. We further analyzed the relationship between the protein expression of the hub genes and the prognosis and the status of immune cell infiltration in PAAD.

We identified 4 circRNAs, *circ-UBAP2*, *circ-CLEC17A*, *circ-HIBADH* and *circ-TADA2A*, as part of the ceRNA network from among 457 DEcircRNAs. Previous studies have shown that *circ-UBAP2* plays an important role in many cancers by acting as a sponge for miRNAs. In triple-negative breast cancer (TNBC), upregulated *circ-UBAP2* binds to and inhibits *miR-661*, which promotes high expression of the *MTA1* oncogene that activates TNBC cell proliferation and migration [20]. In osteosarcoma cells, *circ-UBAP2* acts as an *miR-143* sponge and suppresses apoptosis by upregulating *Bcl-2* [21]. The role of *circ-UBAP2* in PAAD has not been reported. Our study suggests that up-regulated *circ-UBAP2* inhibits the expression of *hsa-miR-494* to promote pancreatic tumorigenesis. The roles of *circ-CLEC17A*, *circ-HIBADH* and *circ-TADA2A* in tumorigenesis have not been previously reported. Our results indicate that the *circ-CLEC17A*/*hsa-mir-324-3p*, *circ-HIBADH*/*hsa-miR-214* and *circ-TADA2A*/*hsa-miR-214* axis modulate the biogenesis, growth and progression of PAAD. Nevertheless, our data require further experimental confirmation.

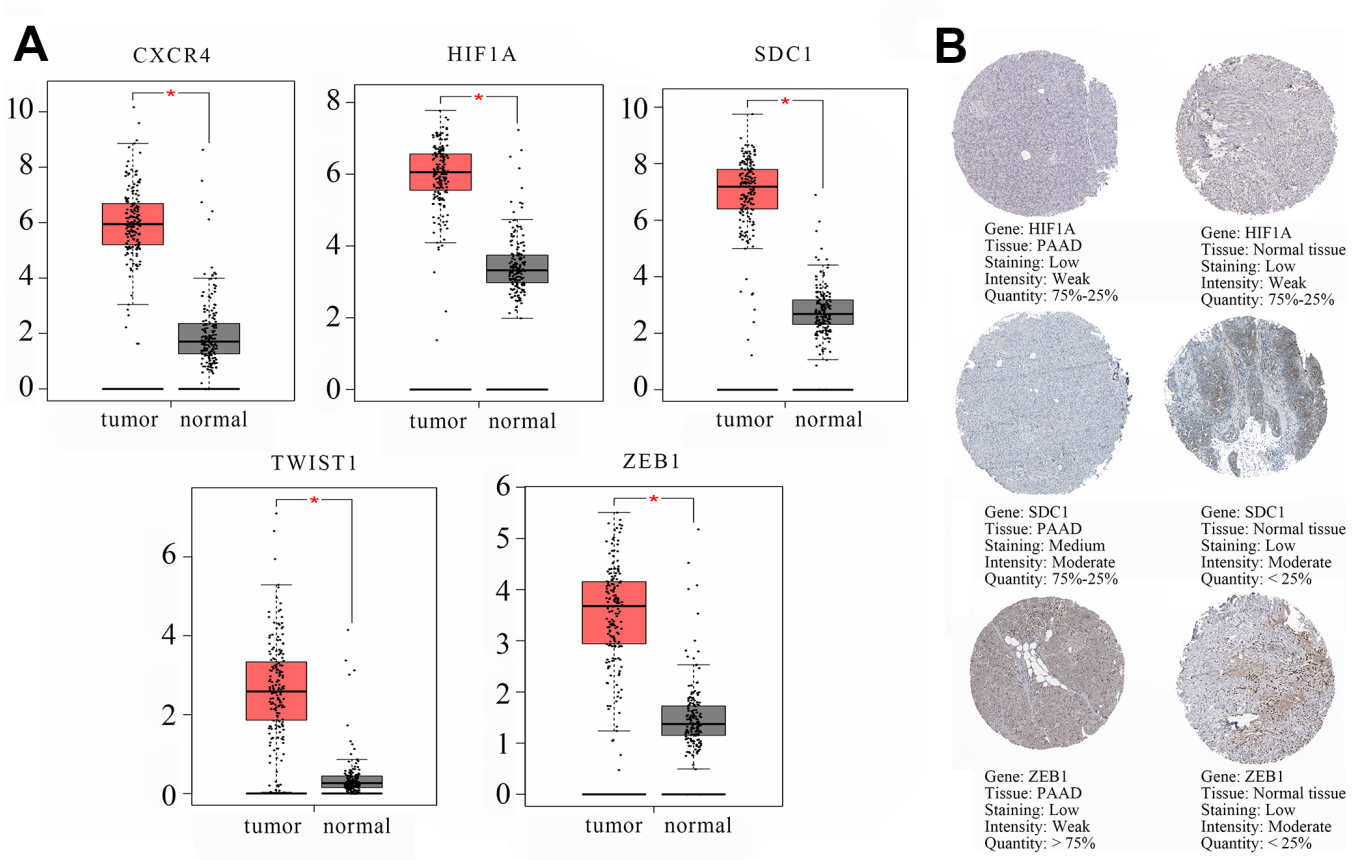

Figure 7. Validation of the transcript (mRNA) and protein levels of the hub genes using the Gene Expression Profiling Interactive Analysis (GEPIA) and The Human Protein Atlas database. (**A**) The transcript (mRNA) of the hub genes, namely, *CXCR4*, *HIF1A*, *SDC1*, *TWIST1*, and *ZEB1* in PAAD and normal pancreatic tissues are shown. (**B**) Immunohistochemical (IHC) staining data of hub genes as follows: *HIF1A* protein expression in a PAAD tumor tissue (Staining: low; Intensity: weak; Quantity: 75%-25%; Location: cytoplasmic/membrane); *HIF1A* protein expression in a representative normal pancreatic tissue (Staining: low; Intensity: weak; Quantity: 75%-25%; Location: nuclear); *SDC1* protein expression in a PAAD tumor tissue (Staining: medium; Intensity: moderate; Quantity: 75%-25%; Location: cytoplasmic/membrane). *SDC1* protein expression in a representative normal pancreatic tissue (Staining: low; Intensity: moderate; Quantity: < 25%; Location: cytoplasmic/membrane). *ZEB1* protein expression in a PAAD tumor tissue (Staining: low; Intensity: weak; Quantity: > 75%; Location: cytoplasmic/membrane). *ZEB1* protein expression in a representative normal pancreatic tissue (Staining: low; Intensity: moderate; Quantity: < 25%; Location: cytoplasmic/membrane). The database lacked information regarding *CXCR4* and *TWIST1* protein expression in PAAD tumor tissues and normal pancreatic tissues. IHC results consistent with changed trend of transcript (mRNA) of hub genes in GSE60980 (GPL14550) and GEPIA were displayed.

We identified 5 hub genes that have previously been associated with PAAD tumorigenesis. Artemin promotes metastasis and invasiveness of PAAD cells by inducing *CXCR4* expression via the activation of the NF-κB signaling [22]. Moreover, *miR-494* inhibits proliferation, invasion and metastasis of prostate and breast cancer cells by suppressing *CXCR4* expression [23, 24]. Furthermore, *miR-494* suppresses epithelial-mesenchymal transition (EMT), metastasis and invasiveness of PAAD cells by downregulating *SDC1* [25]. Liu H et al. reported that downregulation of *TWIST1* suppresses PAAD cell invasiveness and metastasis [26]. *TWIST1* may be a direct target of *hsa-miR-214*, which is part of the ceRNA network we constructed in this study. Cao et al. reported that down-regulation of *mir-214-5p* promotes the proliferation, invasion and migration of PAAD cells in a *JAG1*-dependent manner, which is consistent with the effect of *TWIST1* knockdown [27]. We therefore speculate that the *hsa-miR-214*/*TWIST1* axis plays a critical role in PAAD progression. When exposed to hypoxic conditions, PAAD cells generate exosomes that are rich in *mir-301a-3p* which induces M2 polarization of the tumor-associated macrophages (TAMs) via the activation of PTEN/PI3Kγ in a *HIF1A*- or *HIF2A*-dependent manner, thereby promoting tumor cell EMT, invasiveness, and metastasis [28]. In hypoxic conditions, activated *KRAS* upregulates carbonic anhydrase 9 modulates pH and glycolysis via *HIF1A* or *HIF2A* and promotes aggressive growth of PAAD cells [29]. Notably, 4 out of the 5 hub genes, namely, *CXCR4*, *SDC1*, *ZEB1* and *HIF1A*, are potential targets of the *circ-UBAP2*/*hsa-miR-494* ceRNA network. This suggests that *circ-UBAP2*/*hsa-miR-494* ceRNA network plays a critical role in the initiation, growth, and progression of PAAD.

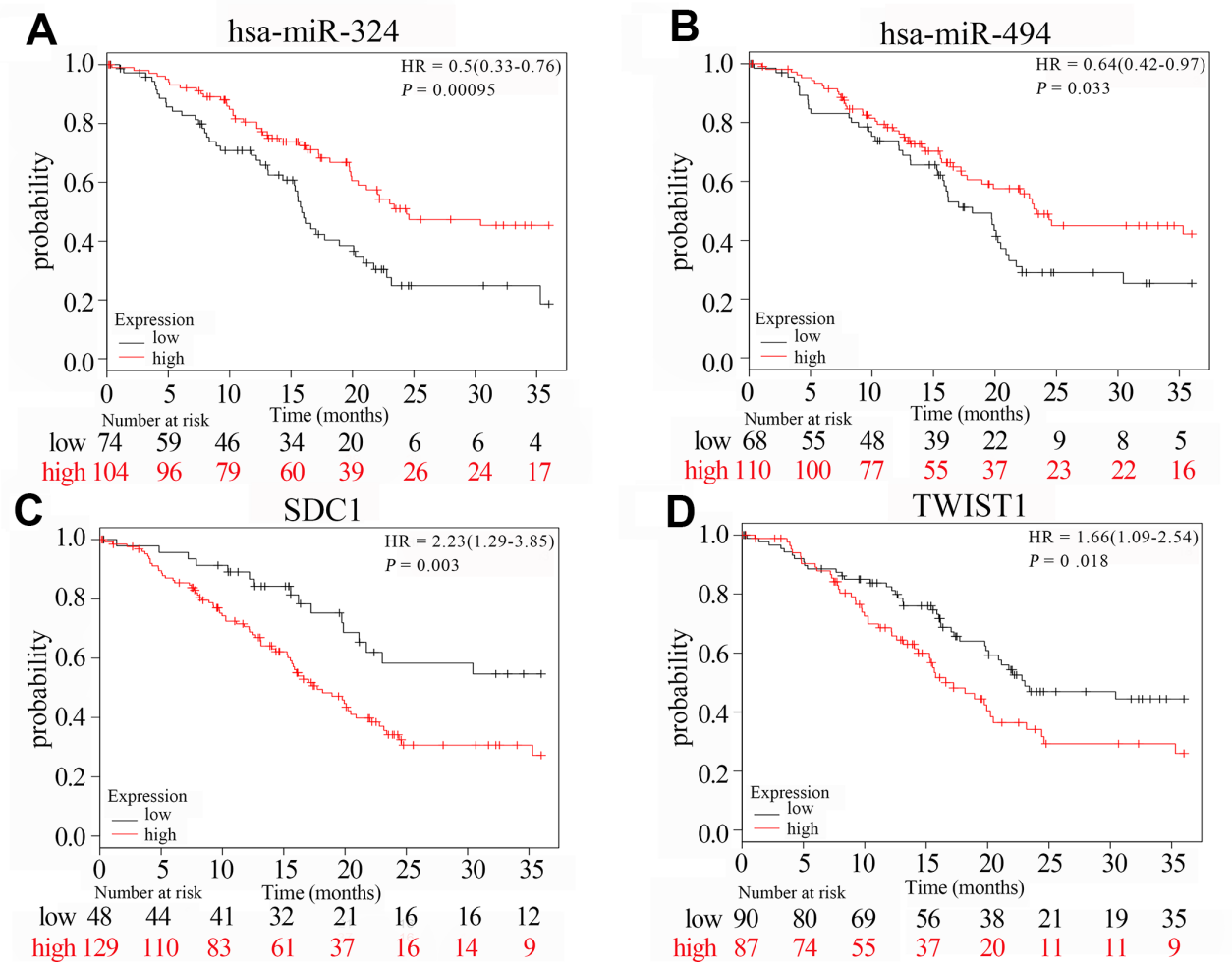

Figure 8. The survival curves of hub genes and their related miRNAs based on Kaplan Meier. (**A**–**D**) Transcription levels of *hsa-miR-324*, *hsa-miR-494*, *SDC1* and *TWIST1* are significantly related to the overall survival of patients with PAAD ($P < 0.05$). Red curve indicates high expression in PAAD tumor tissues; black curve indicates low expression in PAAD tumor tissues; *P* value < 0.05 indicates statistical significance; HR: hazard ratio.

Table 2. Correlation analyses between 5 hub genes and the corresponding markers of immune cells in TIMER.

Description	Gene makers	CXCR4		HIF1A		SDC1		TWIST1		ZEB1	
		Purity		Purity		Purity		Purity		Purity	
		Cor	*P*	Cor	*P*	Cor	*P*	Cor	*P*	Cor	*P*
CD8+ T cell	CD8A	0.667	***	0.265	***	-0.423	***	-0.025	0.749	0.259	***
	CD8B	0.549	***	0.188	*	-0.273	***	-0.039	0.609	0.419	***
T cell (general)	CD3D	0.727	***	0.119	0.120	-0.304	***	0.080	0.299	0.367	***
	CD3E	0.739	***	0.181	*	-0.344	***	0.051	0.510	0.447	***
	CD2	0.711	***	0.207	**	-0.377	***	0.028	0.718	0.465	***
B cell	CD19	0.612	***	0.020	0.800	-0.135	0.077	0.126	0.100	0.352	***
	CD79A	0.610	***	0.102	0.184	-0.147	0.056	0.122	0.112	0.344	***
Monocyte	CD86	0.665	***	0.425	***	-0.273	***	0.321	***	0.552	***
	CD115 (CSF1R)	0.592	***	0.360	***	-0.415	***	0.107	0.163	0.598	***
TAM	CCL2	0.394	***	0.320	***	-0.384	***	0.037	0.629	0.335	***
	CD68	0.386	***	0.319	***	-0.019	0.805	0.280	***	0.253	***
	IL10	0.527	***	0.297	***	-0.230	**	0.250	***	0.501	***
M1 macrophage	INOS (NOS2)	0.193	*	0.128	0.095	-0.091	0.237	0.177	*	0.191	*
	IRF5	0.307	***	-0.152	*	0.081	0.291	0.201	**	0.047	0.540
	COX2(PTGS2)	0.030	0.699	0.292	***	0.226	**	0.281	***	0.224	**
M2 macrophage	CD163	0.541	***	0.424	***	-0.351	***	0.179	*	0.594	***
	VSIG4	0.484	***	0.321	***	-0.349	***	0.213	**	0.472	***
	MS4A4A	0.602	***	0.355	***	-0.393	***	0.202	**	0.579	***
Neutrophils	CD66b (CEACAM8)	0.189	*	0.079	0.303	-0.085	0.269	0.022	0.772	0.099	0.196
	CD11b (ITGAM)	0.490	***	0.238	**	-0.208	**	0.261	***	0.409	***
	CCR7	0.701	***	0.151	*	-0.314	***	0.035	0.647	0.424	***
Natural killer cell	KIR2DL1	0.235	**	0.103	0.180	-0.058	0.450	0.118	0.123	0.147	0.055
	KIR2DL3	0.279	***	0.108	0.158	-0.043	0.577	0.111	0.149	0.185	*
	KIR2DL4	0.056	0.469	0.099	0.197	-0.081	0.290	0.056	0.469	0.001	0.990
	KIR3DL1	0.305	***	0.168	*	-0.253	***	0.029	0.708	0.226	**
	KIR3DL2	0.239	**	0.032	0.679	-0.120	0.119	0.184	*	0.181	*
	KIR3DL3	-0.074	0.334	0.056	0.464	0.043	0.577	0.052	0.500	0.115	0.135
	KIR2DS4	0.073	0.340	0.070	0.360	-0.116	0.132	-0.026	0.733	0.030	0.702
Dendritic cell	HLA-DPB1	0.721	***	0.244	**	-0.306	***	0.146	0.056	0.466	***
	HLA-DQB1	0.457	***	0.171	*	-0.245	**	0.092	0.231	0.295	***
	HLA-DRA	0.685	***	0.341	***	-0.298	***	0.209	**	0.513	***
	HLA-DPA1	0.671	***	0.303	***	-0.320	***	0.147	0.055	0.513	***
	BDCA-1(CD1C)	0.618	***	0.220	**	-0.304	***	0.002	0.987	0.460	***
	BDCA-4(NRP1)	0.376	***	0.645	***	-0.393	***	0.041	0.594	0.660	***
	CD11c (ITGAX)	0.617	***	0.266	**	-0.151	*	0.388	***	0.379	***
Th1	T-bet (TBX21)	0.662	***	0.174	*	-0.386	***	-0.017	0.829	0.372	***
	STAT4	0.602	***	0.229	**	-0.492	***	-0.116	0.132	0.413	***
	STAT1	0.164	*	0.369	***	0.004	0.961	0.115	0.135	0.299	***
	IFN-γ (IFNG)	0.360	***	0.193	*	-0.096	0.213	0.127	0.098	0.223	**
	TNF-α (TNF)	0.409	***	0.106	0.168	-0.155	*	0.265	***	0.168	*
Th2	GATA3	0.175	*	0.064	0.407	0.180	*	0.224	**	0.098	0.204
	STAT6	-0.039	0.610	-0.013	0.869	0.092	0.232	-0.133	0.084	-0.085	0.271
	STAT5A	0.573	***	-0.064	0.402	-0.134	0.079	0.036	0.638	0.243	**
	IL13	0.144	0.060	-0.008	0.915	-0.123	0.109	0.012	0.888	0.144	0.060
Tfh	BCL6	0.264	***	0.447	***	-0.001	0.992	0.223	**	0.260	***
	IL21	0.343	***	0.152	*	-0.176	*	0.082	0.284	0.224	**
Th17	STAT3	0.341	***	0.526	***	-0.305	***	-0.003	0.966	0.563	***

	IL17A	0.108	0.161	0.202	**	-0.259	***	-0.184	*	0.119	0.122
Treg	FOXP3	0.612	***	0.227	**	-0.218	**	0.249	**	0.483	***
	CCR8	0.545	***	0.391	***	-0.242	**	0.182	*	0.585	***
	STAT5B	0.450	***	0.209	**	-0.469	***	-0.042	0.586	0.580	***
	TGFβ (TGFB1)	0.260	***	0.057	0.458	0.213	**	0.504	***	0.135	0.078
T cell exhaustion	PD-1 (PDCD1)	0.631	***	0.207	**	-0.225	**	0.085	0.269	0.327	***
	CTLA4	0.728	***	0.209	**	-0.276	***	0.194	*	0.394	***
	LAG3	0.426	***	0.033	0.673	-0.237	**	0.120	0.118	0.170	*
	TIM-3 (HAVCR2)	0.654	***	0.316	***	-0.239	**	0.330	***	0.492	***
	GZMB	0.484	***	0.214	**	-0.260	***	0.121	0.114	0.277	***

The following categories were used to define correlation strength based on the absolute values : "0.00–0.19" indicates very weak; "0.20–0.39" indicates weak; "0.40–0.59" indicates moderate; "0.60–0.79" indicates strong; "0.80–1.0" indicates very strong; *P* value < 0.05 was defined as statistically significant; Tfh, Follicular helper T cell; Tregs, regulatory T cells; Th, T helper cells; TAM, tumor-associated macrophages; Purity, correlation adjusted by purity; Cor, R-value of Spearman's correlation; * *P* < 0.05; ** *P* < 0.01; *** *P* < 0.001.

To address the potential regulatory roles of the hub genes in the recruitment of tumor-infiltrating lymphocytes, we assessed the correlation between the expression of hub genes and the status of immune infiltration levels in PAAD using the TIMER database. Our data suggest that high expression of both *CXCR4* and *ZEB1* correlates moderately or strongly with the markers of immune cell types such as M2 macrophages, *CD163*, *VSIG4* and *MS4A4A*, but shows a weak correlation with M1 macrophage markers. A previous study confirmed that high expression of *ZEB1* induces polarization of TAMs and promotes ovarian tumor growth [30]. We hypothesize that up-regulated *CXCR4* and *ZEB1* promotes M2 polarization of TAMs and promotes growth and progression of PAAD. Earlier studies have shown that activated Tregs suppress antitumor immunity and promote tumor survival [31]. In this study, Treg markers such as *FOXP3*, *CCR8* and *STAT5B* show a positive correlation with the mRNA levels of *CXCR4* and *ZEB1*. This suggests that *CXCR4* and *ZEB1* expression levels may indicate Treg activity in the tumor microenvironment. Santagata S et al. reported that the tumor suppressive activity of Tregs could be reversed by *CXCR4* inhibition in renal cancer cells [32]. Our results suggest that the high expression level of these two hub genes may contribute to recruitment and activation of Tregs in the PAAD microenvironment.

High expression of *CXCR4* and *ZEB1* correlates positively with critical immune checkpoint proteins such as *PD-1*, *CTLA4* and *TIM-3*. This suggests that high expression of *CXCR4* and *ZEB1* may induce T cell exhaustion and promote immune escape. Consistent with this hypothesis, Seo et al. reported that dual blockade of the *PD-1* and *CXCR4* pathways facilitates PAAD cell apoptosis via CD8+ T cells [33]. Garg et al. reported that NF-κB activity in pancreatic stellate cells induces high expression of *CXCL12*, a ligand of *CXCR4*, and this prevents the tumor infiltration of cytotoxic T cells and impairs their ability to kill tumor cells [34]. Furthermore,

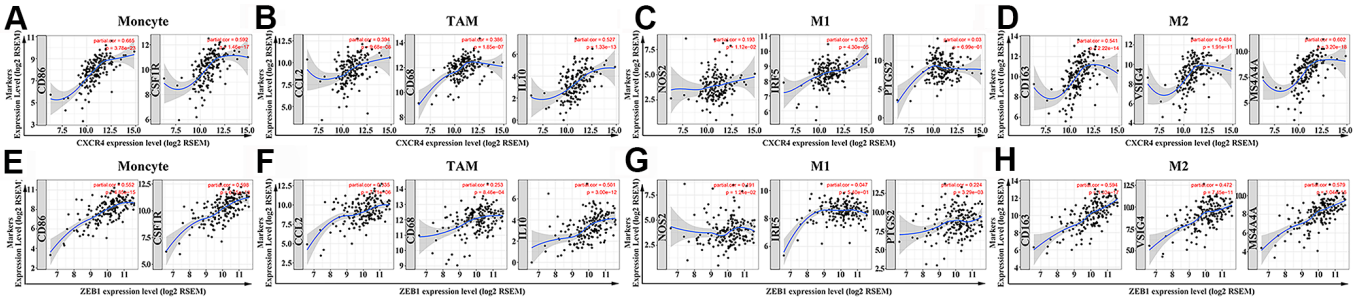

Figure 9. The two hub genes positively correlate with macrophage polarization in PAAD tissues. (**A**–**D**) The relationship between *CXCR4* expression and biomarkers of monocytes, TAMs, M1 and M2 macrophages is shown. (**E**–**H**) The relationship between *ZEB1* expression and biomarkers of monocytes, TAMs, M1 and M2 macrophages is shown. Note: Monocyte markers: *CD86* and *CSF1R*; TAM markers: *CCL2*, *CD68* and IL10; M1 macrophage markers: *NOS2*, *IRF5* and *PTGS2*; M2 macrophage markers: *CD163*, *VSIG4* and *MS4A4A*. Hub genes are shown on the x-axis, and the corresponding marker genes are shown on the y-axis.

CXCR4 inhibitor in combination with an immune-activating fusion protein called VIC-008 suppresses mesothelioma growth by inhibiting *PD-1* expression in CD8+ T cells and promotes transition of Tregs into T helper cells [35]. The upregulation of *PD-1* and *TIM-3* on CD4+ and CD8+ T cells restricts T cell responses in patients with PAAD [36].

In summary, our study demonstrates that circRNAs regulate PAAD by modulating the expression of the hub genes via the ceRNA network. Furthermore, the ceRNA network involving *circ-UBAP2*, *hsa-miR-494* and the 5 hub genes, especially for *CXCR4* and *ZEB1*, regulates PAAD by modulating the tumor infiltration of immune cells.

MATERIALS AND METHODS

Microarray data

In this study, the microarray data of circRNA was obtained from the GSE79634 and GSE69362 datasets. The GSE79634 dataset was based on the GPL19978 platform and included 20 PAAD and adjacent normal tissue samples each. The GSE69362 dataset was based on the GPL19978 platform and contained 6 PAAD and adjacent normal tissue samples each. The microarray data of miRNA was obtained from the GSE60980 (GPL15159) dataset and included 51 PAAD and 6 normal samples. The microarray data of mRNA was obtained from the GSE60980 (GPL14550) dataset and included 49 PAAD and 12 normal samples.

Identification of DEcircRNAs, DEmiRNAs and DEmRNAs

The expression of cicrRNAs in the GSE79634 and GSE69362 datasets was normalized in quantile method, and the DEcircRNAs were determined using the "limma" package [37]. P values < 0.05 and $|\log FC| \geq 1$ were defined as statistically significant. Furthermore, to enhance the accuracy of the results, the DEcircRNAs were analyzed using the Venn diagram software (http://bioinformatics.psb.ugent.be/webtools/Venn/), and the intersections between the various DEcircRNAs were calculated. We used a similar strategy to analyze the differential expression of the miRNAs in GSE60980 (GPL15159) and the mRNAs in GSE60980 (GPL14550).

Construction of the circRNA-miRNA-mRNA network

To construct the circRNA-miRNA-mRNA network, we obtained basic information regarding the circRNAs, including their chromosomal locations from the circBase (http://www.circbase.org) [38]. We then used the cancer-specific circRNA database (CSCD) [39] to establish a circRNA-miRNA network associated with pancreatic tumorigenesis based on the intersection between the circRNA-miRNA pairs and the DEmiRNAs. We also downloaded all the available information of the circRNAs from the CSCD, including the number and the position of the microRNA response element (MRE), the RNA binding protein (RBP) and the open reading frame (ORF). Next, we obtained the miRNA-predicted mRNA pairs from the miRDB, miRTarBase and TargetScan databases, and made an intersection between the predicted mRNAs and the DEmRNAs to construct a miRNA-mRNA network related to pancreatic tumorigenesis. In the three databases, these predicted miRNA-mRNA pairs are validated experimentally by reporter assay, western blot, microarray and next-generation sequencing experiments. Only pairs existed in at least 2 out of 3 databases mentioned before were thought stable and would be included in the present study [40–42]. Finally, we constructed a visual display of the circRNA-miRNA-mRNA network using the Cytoscape software [43].

Analysis of DEmRNAs

We performed GO enrichment analysis of the DEmRNAs to identify biological processes involved in pancreatic tumorigenesis using DAVID (version 6.8, Database for Annotation, Visualization and Integrated Discovery, https://david.ncifcrf.gov/) [44].

KEGG enrichment analysis was performed by the Gene Set Enrichment Analysis (GSEA) method using the "clusterprofiler" package [45]. Biological processes (BP) and KEGG pathways with a P value < 0.05 were considered statistically significant and visualized as a Sankey plot using the "ggalluvial" package [46].

Identification and validation of the hub genes

We analyzed the relative importance of the DEmRNAs using the STRING database (https://string-db.org/) [47], which contains 9,643,763 proteins from 2,031 organisms and 1,380,838,440 interactions. We constructed the PPI network using the Cytoscape software. The genes were ranked using the cytoHubba plug-in in Cytoscape [48]. We identified the hub genes by integrating the results of the GO, KEGG and PPI network analyses. The expression of 4 circRNAs (*circ-HIBADH*, *circ-UBAP2*, *circ-TADA2A*, and *circ-CLEC17A*), 3 miRNAs (*has-miR-214*, *has-mir-324-3p*, and *has-miR-494*) and 5 hub genes (*CXCR4*,*HIF1A*, *ZEB1*, *SDC1* and *TWIST1*) were compared between the PAAD and the normal pancreatic tissues from the GEO dataset. The GEPIA (http://gepia.cancer-pku.cn/) [49] and THPA database (https://www.proteinatlas.org) [50] were used to validate

the transcript (mRNA) and the protein levels of the hub genes. Differentially expressed genes were identified by applying the criteria of |log 2 FC| > 1 and P value < 0.05. Moreover, we compared the expression of the four circRNAs in men and women using the GSE79634 database that provides gender-based information for PAAD patients.

Analysis of the hub genes

We plotted survival curve in KM plotter database (http://kmplot.com/analysis/) [51] to explore connections between overall survival (OS) and *5* hub genes (*CXCR4*, *HIF1A*, *ZEB1*, *SDC1* and *TWIST1)* as well as 3 miRNAs (*has-miR-214*, *has-mir-324-3p*, and *has-miR-494*) in the ceRNA network. Parameters as follows: split patients by "auto select best cutoff", follow up threshold = 36 months, cancer type: pancreatic ductal adenocarcinoma. Significant results with *P* value < 0.05 were recoded.

The hub genes in the ceRNA network were then analyzed by the TIMER database (https://cistrome.shinyapps.io/timer/) [52] to detect immune cell infiltration using various immune markers. The gene modules identified tumor-infiltrating immune cells such as B cells, CD4+ T cells, CD8+ T cells, neutrophils, macrophages, and DCs. The correlation modules identified the gene markers for CD8+ T cells, T cells (general), B cells, monocytes, TAMs, M1 and M2 macrophages, neutrophils, NK cells, DCs cells, Th1 cells, Th2 cells, Tfhs, Th17s cells, Tregs, and exhausted T cells that were previously reported [53]. The power of the correlation was determined as follows: "0.00–0.19" indicated very weak, "0.20–0.39" indicated weak, "0.40–0.59" indicated moderate, "0.60–0.79" indicated strong, and "0.80–1.0" indicated very strong.

AUTHOR CONTRIBUTIONS

Conceptualization: WD. H, HM. P; Experiments: RJ. Z, JJ. N, S. L, LK. Y, JW. S, CY. Z, W. Z, SP. S; Data analysis: RJ. Z, SJ. J, H. L; Original draft writing: RJ. Z, WD. H; Review, editing, and final approval: RJ. Z, WD. H; Research supervision: WD. H, HM.P.

CONFLICTS OF INTEREST

The authors declare that there are no conflicts of interest.

FUNDING

This work was supported by the grants from the Zhejiang Natural Sciences Foundation (LQ18H160008, LQ17H160011, and LY17H160029), the Ten Thousand Plan Youth Talent Support Program of Zhejiang Province, the Zhejiang Medical and Health Science and Technology Project (2016KYB290, 2016ZDB007, and 2017ZD021), the Zhejiang Medical Innovative Discipline Construction Project-2016, and the Hangzhou Health and Family planning and Science and Technology Project (OO20190347).

REFERENCES

1. Bray F, Ferlay J, Soerjomataram I, Siegel RL, Torre LA, Jemal A. Global cancer statistics 2018: GLOBOCAN estimates of incidence and mortality worldwide for 36 cancers in 185 countries. CA Cancer J Clin. 2018; 68:394–424. https://doi.org/10.3322/caac.21492 PMID:30207593

2. Aier I, Semwal R, Sharma A, Varadwaj PK. A systematic assessment of statistics, risk factors, and underlying features involved in pancreatic cancer. Cancer Epidemiol. 2019; 58:104–10. https://doi.org/10.1016/j.canep.2018.12.001 PMID:30537645

3. Mahmood J, Shukla HD, Soman S, Samanta S, Singh P, Kamlapurkar S, Saeed A, Amin NP, Vujaskovic Z. Immunotherapy, Radiotherapy, and Hyperthermia: A Combined Therapeutic Approach in Pancreatic Cancer Treatment. Cancers (Basel). 2018; 10:469. https://doi.org/10.3390/cancers10120469 PMID:30486519

4. Biancur DE, Kimmelman AC. The plasticity of pancreatic cancer metabolism in tumor progression and therapeutic resistance. Biochim Biophys Acta Rev Cancer. 2018; 1870:67–75. https://doi.org/10.1016/j.bbcan.2018.04.011 PMID:29702208

5. Li Z, Tao Y, Wang X, Jiang P, Li J, Peng M, Zhang X, Chen K, Liu H, Zhen P, Zhu J, Liu X, Liu X. Tumor-Secreted Exosomal miR-222 Promotes Tumor Progression via Regulating P27 Expression and Re-Localization in Pancreatic Cancer. Cell Physiol Biochem. 2018; 51:610–29. https://doi.org/10.1159/000495281 PMID:30458449

6. Chen S, Chen JZ, Zhang JQ, Chen HX, Qiu FN, Yan ML, Tian YF, Peng CH, Shen BY, Chen YL, Wang YD. Silencing of long noncoding RNA LINC00958 prevents tumor initiation of pancreatic cancer by acting as a sponge of microRNA-330-5p to down-regulate PAX8. Cancer Lett. 2019; 446:49–61. https://doi.org/10.1016/j.canlet.2018.12.017 PMID:30639194

7. Bolha L, Ravnik-Glavač M, Glavač D. Circular RNAs: Biogenesis, Function, and a Role as Possible Cancer Biomarkers. Int J Genomics. 2017; 2017:6218353. https://doi.org/10.1155/2017/6218353 PMID:29349062

8. Sanger HL, Klotz G, Riesner D, Gross HJ, Kleinschmidt AK. Viroids are single-stranded covalently closed circular RNA molecules existing as highly base-paired rod-like structures. Proc Natl Acad Sci USA. 1976; 73:3852–56. https://doi.org/10.1073/pnas.73.11.3852 PMID:1069269

9. Wang Y, Mo Y, Gong Z, Yang X, Yang M, Zhang S, Xiong F, Xiang B, Zhou M, Liao Q, Zhang W, Li X, Li X, et al. Circular RNAs in human cancer. Mol Cancer. 2017; 16:25. https://doi.org/10.1186/s12943-017-0598-7 PMID:28143578

10. Chen S, Zhao Y. Circular RNAs: Characteristics, function, and role in human cancer. Histol Histopathol. 2018; 33:887–93. https://doi.org/10.14670/HH-11-969 PMID:29393503

11. Li J, Li Z, Jiang P, Peng M, Zhang X, Chen K, Liu H, Bi H, Liu X, Li X. Circular RNA IARS (circ-IARS) secreted by pancreatic cancer cells and located within exosomes regulates endothelial monolayer permeability to promote tumor metastasis. J Exp Clin Cancer Res. 2018; 37:177. https://doi.org/10.1186/s13046-018-0822-3 PMID:30064461

12. Zhong Y, Du Y, Yang X, Mo Y, Fan C, Xiong F, Ren D, Ye X, Li C, Wang Y, Wei F, Guo C, Wu X, et al. Circular RNAs function as ceRNAs to regulate and control human cancer progression. Mol Cancer. 2018; 17:79. https://doi.org/10.1186/s12943-018-0827-8 PMID:29626935

13. Feng C, Li Y, Lin Y, Cao X, Li D, Zhang H, He X. CircRNA-associated ceRNA network reveals ErbB and Hippo signaling pathways in hypopharyngeal cancer. Int J Mol Med. 2019; 43:127–42. https://doi.org/10.3892/ijmm.2018.3942 PMID:30365065

14. Gardian K, Janczewska S, Durlik M. Microenvironment elements involved in the development of pancreatic cancer tumor. Gastroenterol Res Pract. 2012; 2012:585674. https://doi.org/10.1155/2012/585674 PMID:23304126

15. Qu S, Song W, Yang X, Wang J, Zhang R, Zhang Z, Zhang H, Li H. Microarray expression profile of circular RNAs in human pancreatic ductal adenocarcinoma. Genom Data. 2015; 5:385–87. https://doi.org/10.1016/j.gdata.2015.07.017 PMID:26484292

16. Guo S, Xu X, Ouyang Y, Wang Y, Yang J, Yin L, Ge J, Wang H. Microarray expression profile analysis of circular RNAs in pancreatic cancer. Mol Med Rep. 2018; 17:7661–71. https://doi.org/10.3892/mmr.2018.8827 PMID:29620241

17. Fujioka S, Sclabas GM, Schmidt C, Niu J, Frederick WA, Dong QG, Abbruzzese JL, Evans DB, Baker C, Chiao PJ. Inhibition of constitutive NF-kappa B activity by I kappa B alpha M suppresses tumorigenesis. Oncogene. 2003; 22:1365–70. https://doi.org/10.1038/sj.onc.1206323 PMID:12618762

18. Xue R, Meng Q, Lu D, Liu X, Wang Y, Hao J. Mitofusin2 Induces Cell Autophagy of Pancreatic Cancer through Inhibiting the PI3K/Akt/mTOR Signaling Pathway. Oxid Med Cell Longev. 2018; 2018:2798070. https://doi.org/10.1155/2018/2798070 PMID:30046371

19. Garg B, Giri B, Majumder K, Dudeja V, Banerjee S, Saluja A. Modulation of post-translational modifications in β-catenin and LRP6 inhibits Wnt signaling pathway in pancreatic cancer. Cancer Lett. 2017; 388:64–72. https://doi.org/10.1016/j.canlet.2016.11.026 PMID:27919787

20. Wang S, Li Q, Wang Y, Li X, Wang R, Kang Y, Xue X, Meng R, Wei Q, Feng X. Upregulation of circ-UBAP2 predicts poor prognosis and promotes triple-negative breast cancer progression through the miR-661/MTA1 pathway. Biochem Biophys Res Commun. 2018; 505:996–1002. https://doi.org/10.1016/j.bbrc.2018.10.026 PMID:30314706

21. Zhang H, Wang G, Ding C, Liu P, Wang R, Ding W, Tong D, Wu D, Li C, Wei Q, Zhang X, Li D, Liu P, et al. Increased circular RNA UBAP2 acts as a sponge of miR-143 to promote osteosarcoma progression. Oncotarget. 2017; 8:61687–97. https://doi.org/10.18632/oncotarget.18671 PMID:28977896

22. Wang J, Wang H, Cai J, Du S, Xin B, Wei W, Zhang T, Shen X. Artemin regulates CXCR4 expression to induce migration and invasion in pancreatic cancer cells through activation of NF-κB signaling. Exp Cell Res. 2018; 365:12–23. https://doi.org/10.1016/j.yexcr.2018.02.008 PMID:29453972

23. Shen PF, Chen XQ, Liao YC, Chen N, Zhou Q, Wei Q, Li X, Wang J, Zeng H. MicroRNA-494-3p targets CXCR4 to suppress the proliferation, invasion, and migration of prostate cancer. Prostate. 2014; 74:756–67. https://doi.org/10.1002/pros.22795 PMID:24644030

24. Song L, Liu D, Wang B, He J, Zhang S, Dai Z, Ma X, Wang X. miR-494 suppresses the progression of breast cancer in vitro by targeting CXCR4 through the Wnt/β-catenin

signaling pathway. Oncol Rep. 2015; 34:525–31. https://doi.org/10.3892/or.2015.3965 PMID:25955111

25. Yang Y, Tao X, Li CB, Wang CM. MicroRNA-494 acts as a tumor suppressor in pancreatic cancer, inhibiting epithelial-mesenchymal transition, migration and invasion by binding to SDC1. Int J Oncol. 2018; 53:1204–14. https://doi.org/10.3892/ijo.2018.4445 PMID:29956739

26. Liu H, Wang H, Liu X, Yu T. miR-1271 inhibits migration, invasion and epithelial-mesenchymal transition by targeting ZEB1 and TWIST1 in pancreatic cancer cells. Biochem Biophys Res Commun. 2016; 472:346–52. https://doi.org/10.1016/j.bbrc.2016.02.096 PMID:26940738

27. Cao TH, Ling X, Chen C, Tang W, Hu DM, Yin GJ. Role of miR-214-5p in the migration and invasion of pancreatic cancer cells. Eur Rev Med Pharmacol Sci. 2018; 22:7214–21. https://doi.org/10.26355/eurrev_201811_16255 PMID:30468464

28. Wang X, Luo G, Zhang K, Cao J, Huang C, Jiang T, Liu B, Su L, Qiu Z. Hypoxic Tumor-Derived Exosomal miR-301a Mediates M2 Macrophage Polarization via PTEN/PI3Kγ to Promote Pancreatic Cancer Metastasis. Cancer Res. 2018; 78:4586–98. https://doi.org/10.1158/0008-5472.CAN-17-3841 PMID:29880482

29. McDonald PC, Chafe SC, Brown WS, Saberi S, Swayampakula M, Venkateswaran G, Nemirovsky O, Gillespie JA, Karasinska JM, Kalloger SE, Supuran CT, Schaeffer DF, Bashashati A, et al. Regulation of pH by Carbonic Anhydrase 9 Mediates Survival of Pancreatic Cancer Cells With Activated KRAS in Response to Hypoxia. Gastroenterology. 2019; 157:823–37. https://doi.org/10.1053/j.gastro.2019.05.004 PMID:31078621

30. Cortés M, Sanchez-Moral L, de Barrios O, Fernández-Aceñero MJ, Martínez-Campanario MC, Esteve-Codina A, Darling DS, Győrffy B, Lawrence T, Dean DC, Postigo A. Tumor-associated macrophages (TAMs) depend on ZEB1 for their cancer-promoting roles. EMBO J. 2017; 36:3336–55. https://doi.org/10.15252/embj.201797345 PMID:29038174

31. Rani A, Murphy JJ. STAT5 in Cancer and Immunity. J Interferon Cytokine Res. 2016; 36:226–37. https://doi.org/10.1089/jir.2015.0054 PMID:26716518

32. Santagata S, Napolitano M, D'Alterio C, Desicato S, Maro SD, Marinelli L, Fragale A, Buoncervello M, Persico F, Gabriele L, Novellino E, Longo N, Pignata S, et al. Targeting CXCR4 reverts the suppressive activity of T-regulatory cells in renal cancer. Oncotarget. 2017; 8:77110–20. https://doi.org/10.18632/oncotarget.20363 PMID:29100374

33. Seo YD, Jiang X, Sullivan KM, Jalikis FG, Smythe KS, Abbasi A, Vignali M, Park JO, Daniel SK, Pollack SM, Kim TS, Yeung R, Crispe IN, et al. Mobilization of CD8$^+$ T Cells via CXCR4 Blockade Facilitates PD-1 Checkpoint Therapy in Human Pancreatic Cancer. Clin Cancer Res. 2019; 25:3934–45. https://doi.org/10.1158/1078-0432.CCR-19-0081 PMID:30940657

34. Garg B, Giri B, Modi S, Sethi V, Castro I, Umland O, Ban Y, Lavania S, Dawra R, Banerjee S, Vickers S, Merchant NB, Chen SX, et al. NFκB in Pancreatic Stellate Cells Reduces Infiltration of Tumors by Cytotoxic T Cells and Killing of Cancer Cells, via Up-regulation of CXCL12. Gastroenterology. 2018; 155:880–891.e8. https://doi.org/10.1053/j.gastro.2018.05.051 PMID:29909021

35. Li B, Zeng Y, Reeves PM, Ran C, Liu Q, Qu X, Liang Y, Liu Z, Yuan J, Leblanc PR, Ye Z, Sluder AE, Gelfand JA, et al. AMD3100 Augments the Efficacy of Mesothelin-Targeted, Immune-Activating VIC-008 in Mesothelioma by Modulating Intratumoral Immunosuppression. Cancer Immunol Res. 2018; 6:539–51. https://doi.org/10.1158/2326-6066.CIR-17-0530 PMID:29511032

36. Shindo Y, Hazama S, Suzuki N, Iguchi H, Uesugi K, Tanaka H, Aruga A, Hatori T, Ishizaki H, Umeda Y, Fujiwara T, Ikemoto T, Shimada M, et al. Predictive biomarkers for the efficacy of peptide vaccine treatment: based on the results of a phase II study on advanced pancreatic cancer. J Exp Clin Cancer Res. 2017; 36:36. https://doi.org/10.1186/s13046-017-0509-1 PMID:28241889

37. Ritchie ME, Phipson B, Wu D, Hu Y, Law CW, Shi W, Smyth GK. limma powers differential expression analyses for RNA-sequencing and microarray studies. Nucleic Acids Res. 2015; 43:e47. https://doi.org/10.1093/nar/gkv007 PMID:25605792

38. Glažar P, Papavasileiou P, Rajewsky N. circBase: a database for circular RNAs. RNA. 2014; 20:1666–70. https://doi.org/10.1261/rna.043687.113 PMID:25234927

39. Xia S, Feng J, Chen K, Ma Y, Gong J, Cai F, Jin Y, Gao Y, Xia L, Chang H, Wei L, Han L, He C. CSCD: a database for cancer-specific circular RNAs. Nucleic Acids Res. 2018; 46:D925–29. https://doi.org/10.1093/nar/gkx863 PMID:29036403

40. Agarwal V, Bell GW, Nam JW, Bartel DP. Predicting effective microRNA target sites in mammalian mRNAs. eLife. 2015; 4: e05005. https://doi.org/10.7554/eLife.05005 PMID:26267216

41. Chou CH, Shrestha S, Yang CD, Chang NW, Lin YL, Liao KW, Huang WC, Sun TH, Tu SJ, Lee WH, Chiew MY, Tai CS, Wei TY, et al. miRTarBase update 2018: a resource for experimentally validated microRNA-target interactions. Nucleic Acids Res. 2018; 46:D296–302. https://doi.org/10.1093/nar/gkx1067 PMID:29126174

42. Wang X. Improving microRNA target prediction by modeling with unambiguously identified microRNA-target pairs from CLIP-ligation studies. Bioinformatics. 2016; 32:1316–22. https://doi.org/10.1093/bioinformatics/btw002 PMID:26743510

43. Shannon P, Markiel A, Ozier O, Baliga NS, Wang JT, Ramage D, Amin N, Schwikowski B, Ideker T. Cytoscape: a software environment for integrated models of biomolecular interaction networks. Genome Res. 2003; 13:2498–504. https://doi.org/10.1101/gr.1239303 PMID:14597658

44. Huang W, Sherman BT, Lempicki RA. Systematic and integrative analysis of large gene lists using DAVID bioinformatics resources. Nat Protoc. 2009; 4:44–57. https://doi.org/10.1038/nprot.2008.211 PMID:19131956

45. Yu G, Wang LG, Han Y, He QY. clusterProfiler: an R package for comparing biological themes among gene clusters. OMICS. 2012; 16:284–87. https://doi.org/10.1089/omi.2011.0118 PMID:22455463

46. Brunson JC. ggalluvial: Alluvial Diagrams in 'ggplot2'. 2019.

47. Szklarczyk D, Morris JH, Cook H, Kuhn M, Wyder S, Simonovic M, Santos A, Doncheva NT, Roth A, Bork P, Jensen LJ, von Mering C. The STRING database in 2017: quality-controlled protein-protein association networks, made broadly accessible. Nucleic Acids Res. 2017; 45:D362–68. https://doi.org/10.1093/nar/gkw937 PMID:27924014

48. Chin CH, Chen SH, Wu HH, Ho CW, Ko MT, Lin CY. cytoHubba: identifying hub objects and sub-networks from complex interactome. BMC Syst Biol. 2014 (Suppl 4); 8:S11. https://doi.org/10.1186/1752-0509-8-S4-S11 PMID:25521941

49. Tang Z, Li C, Kang B, Gao G, Li C, Zhang Z. GEPIA: a web server for cancer and normal gene expression profiling and interactive analyses. Nucleic Acids Res. 2017; 45:W98–102. https://doi.org/10.1093/nar/gkx247 PMID:28407145

50. Uhlen M, Zhang C, Lee S, Sjöstedt E, Fagerberg L, Bidkhori G, Benfeitas R, Arif M, Liu Z, Edfors F, Sanli K, von Feilitzen K, Oksvold P, et al. A pathology atlas of the human cancer transcriptome. Science. 2017; 357: eaan2507. https://doi.org/10.1126/science.aan2507 PMID:28818916

51. Lánczky A, Nagy Á, Bottai G, Munkácsy G, Szabó A, Santarpia L, Győrffy B. miRpower: a web-tool to validate survival-associated miRNAs utilizing expression data from 2178 breast cancer patients. Breast Cancer Res Treat. 2016; 160:439–46. https://doi.org/10.1007/s10549-016-4013-7 PMID:27744485

52. Li T, Fan J, Wang B, Traugh N, Chen Q, Liu JS, Li B, Liu XS. TIMER: A Web Server for Comprehensive Analysis of Tumor-Infiltrating Immune Cells. Cancer Res. 2017; 77:e108–10. https://doi.org/10.1158/0008-5472.CAN-17-0307 PMID:29092952

53. Pan JH, Zhou H, Cooper L, Huang JL, Zhu SB, Zhao XX, Ding H, Pan YL, Rong L. LAYN Is a Prognostic Biomarker and Correlated With Immune Infiltrates in Gastric and Colon Cancers. Front Immunol. 2019; 10:6. https://doi.org/10.3389/fimmu.2019.00006 PMID:30761122

SUPPLEMENTARY MATERIALS

Supplementary Figures

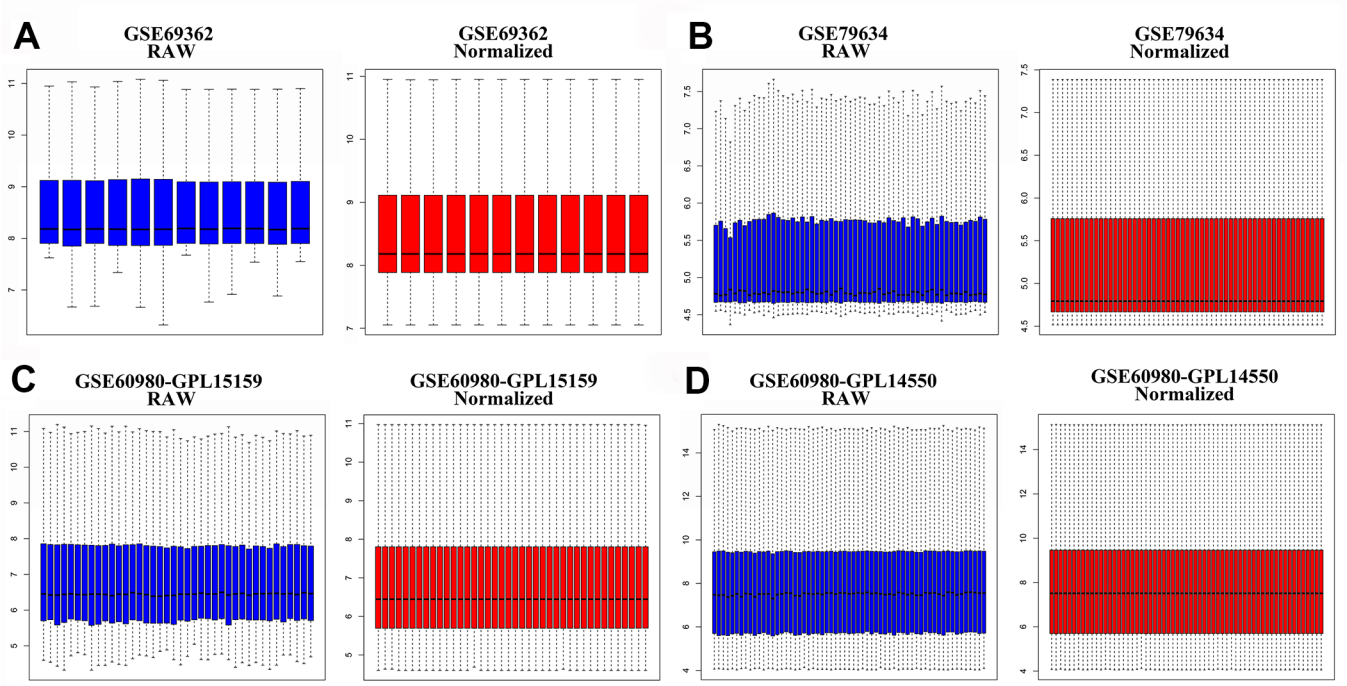

Supplementary Figure 1. Quality control of microarray data of circRNA, microRNA and mRNA. (**A**, **B**) The boxplots show the variations in the expression of circRNAs in the (**A**) GSE69362 and (**B**) GSE79634 datasets and their normalized data. (**C**, **D**) The boxplots show the variations in the expression of (**C**) microRNAs in the GSE60980 (GPL15159) dataset and (**D**) mRNAs in the GSE60980 (GPL14550) dataset and their normalized data.

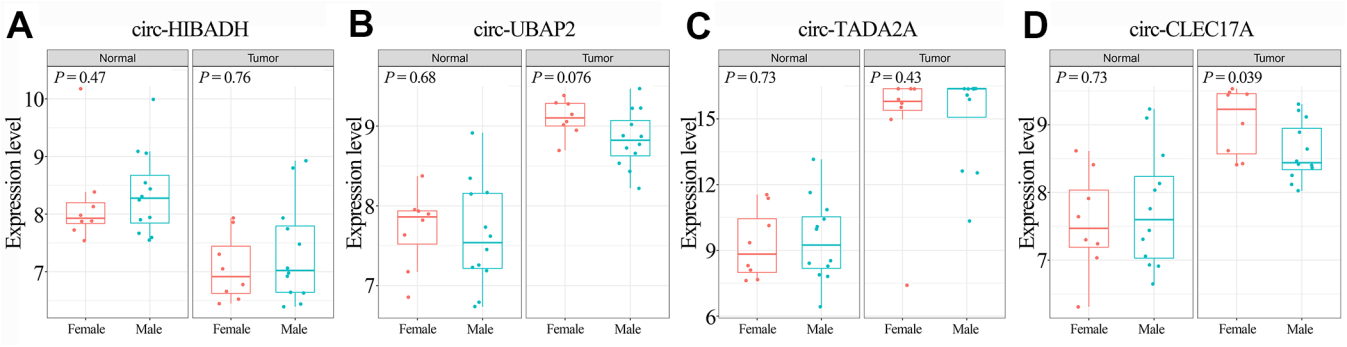

Supplementary Figure 2 Comparative analyses of the transcription levels of circRNAs between females and males in GSE69362. (**A**–**D**) Transcription levels of *circ-HIBADH*, *circ-UBAP2*, *circ-TADA2A*, and *circ-CLEC17A* in GSE69362 between females (red) and males (blue) in PAAD tumor tissues and normal pancreatic tissues.

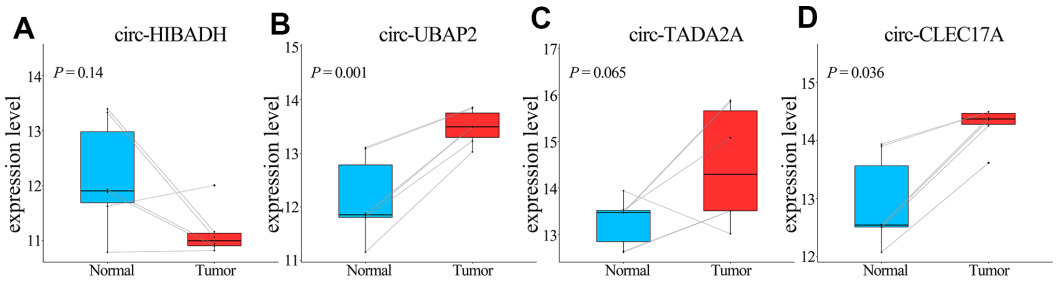

Supplementary Figure 3. Comparative analyses of the transcription levels of circRNAs between PAAD tumor tissues and normal pancreatic tissues in GSE69362. (**A**–**D**) Transcription levels of *circ-HIBADH*, *circ-UBAP2*, *circ-TADA2A* and *circ-CLEC17A* between PAAD tumor tissues (red) and normal pancreatic tissues (blue).

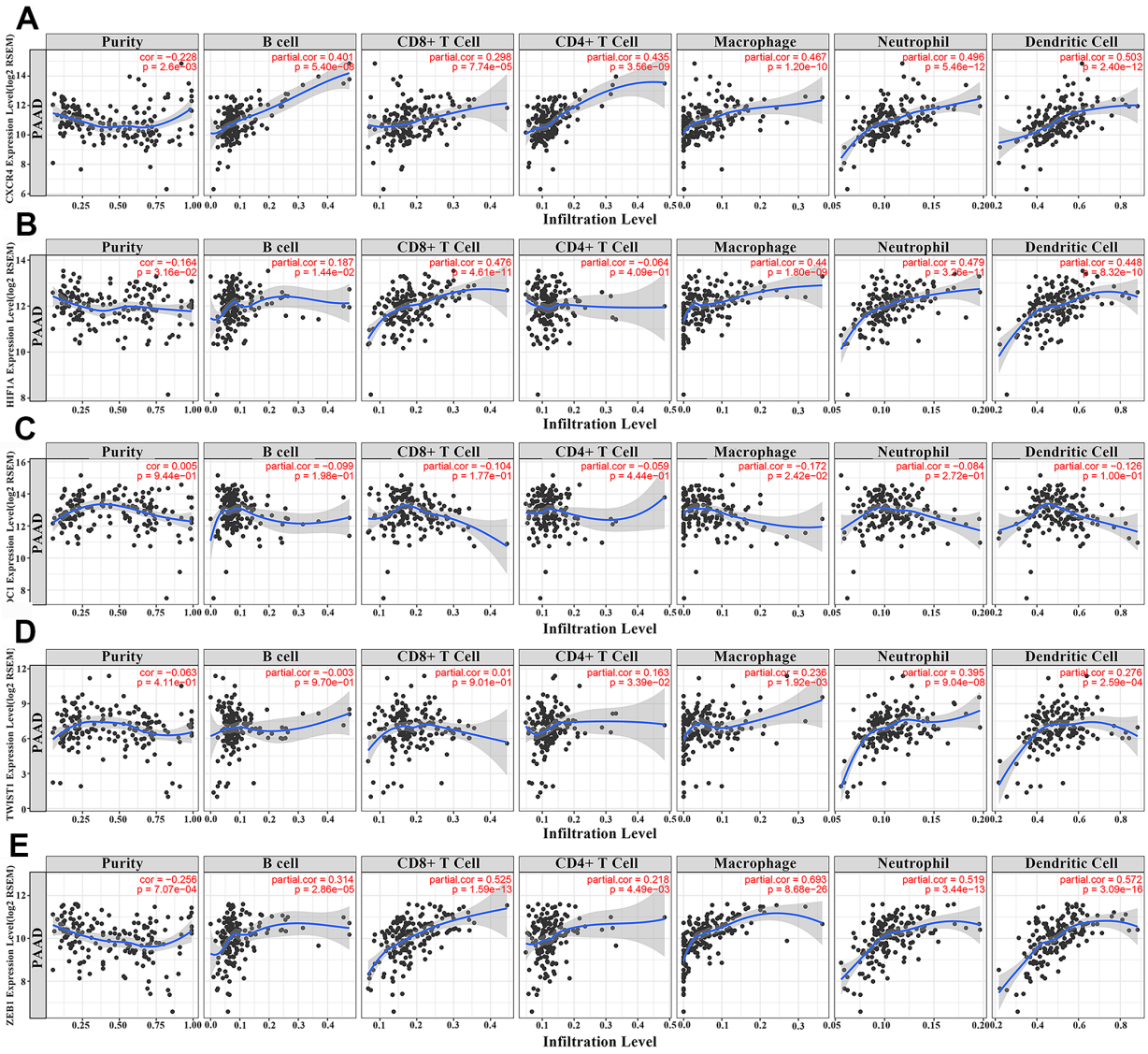

Supplementary Figure 4. The correlation between transcription levels of hub genes and the level of immune cell infiltration. The abscissa represents the abundance of immune cell infiltration, and the ordinate represents the transcription levels of the hub genes. The first column shows the correlation between transcription levels of hub genes and the purity of cancer cells. Columns from 2–7 show the purity-adjusted correlation between the transcription levels of hub genes and six different immune cells, including B cells, CD4 + T cells, CD8 + T cells, neutrophils, macrophages and dendritic cells. Hub genes: (**A**) *CXCR4*, (**B**) *HIF1A*, (**C**) *SDC1*, (**D**) *TWIST1*, (**E**) *ZEB1*.